Applied and Environmental Microbiology, Oct. 2010, p. 6778–6786 Vol. 76, No. 20
0099-2240/10/$12.00 doi:10.1128/AEM.01097-10

Significant Association between Sulfate-Reducing Bacteria and Uranium-Reducing Microbial Communities as Revealed by a Combined Massively Parallel Sequencing-Indicator Species Approach▽†

Erick Cardenas,[1] Wei-Min Wu,[2] Mary Beth Leigh,[1]‡ Jack Carley,[3] Sue Carroll,[3] Terry Gentry,[3]§ Jian Luo,[2]¶ David Watson,[3] Baohua Gu,[3] Matthew Ginder-Vogel,[2]‖ Peter K. Kitanidis,[2] Philip M. Jardine,[3] Jizhong Zhou,[3]# Craig S. Criddle,[2] Terence L. Marsh,[1]* and James M. Tiedje[1]*

Center for Microbial Ecology, Michigan State University, East Lansing, Michigan 48824[1]; Department of Civil and Environmental Engineering, Stanford University, Stanford, California 94305-4020[2]; and Environmental Sciences Division, Oak Ridge National Laboratory, Oak Ridge, Tennessee 37831[3]

Received 6 May 2010/Accepted 12 August 2010

Massively parallel sequencing has provided a more affordable and high-throughput method to study microbial communities, although it has mostly been used in an exploratory fashion. We combined pyrosequencing with a strict indicator species statistical analysis to test if bacteria specifically responded to ethanol injection that successfully promoted dissimilatory uranium(VI) reduction in the subsurface of a uranium contamination plume at the Oak Ridge Field Research Center in Tennessee. Remediation was achieved with a hydraulic flow control consisting of an inner loop, where ethanol was injected, and an outer loop for flow-field protection. This strategy reduced uranium concentrations in groundwater to levels below 0.126 μM and created geochemical gradients in electron donors from the inner-loop injection well toward the outer loop and downgradient flow path. Our analysis with 15 sediment samples from the entire test area found significant indicator species that showed a high degree of adaptation to the three different hydrochemical-created conditions. *Castellaniella* and *Rhodanobacter* characterized areas with low pH, heavy metals, and low bioactivity, while sulfate-, Fe(III)-, and U(VI)-reducing bacteria (*Desulfovibrio*, *Anaeromyxobacter*, and *Desulfosporosinus*) were indicators of areas where U(VI) reduction occurred. The abundance of these bacteria, as well as the Fe(III) and U(VI) reducer *Geobacter*, correlated with the hydraulic connectivity to the substrate injection site, suggesting that the selected populations were a direct response to electron donor addition by the groundwater flow path. A false-discovery-rate approach was implemented to discard false-positive results by chance, given the large amount of data compared.

Massively parallel sequencing has increased our ability to study microbial communities to a greater depth and at decreased sequencing costs to an extent that replication and gradient interrogation are now reasonably attainable. However, this massive throughput has mostly been used in exploratory studies, given the challenges to analysis of the big data sets generated and the relative novelty of the technique. To date, no report of a study that has used this method to describe the microbial community over a large area influenced by complicated hydrogeochemical factors during bioremediation has been published. Here, we used pyrosequencing technology complemented with a hypothesis-based approach to identify bacteria associated with biostimulation of U(VI) reduction at Area 3 of the U.S. Department of Energy's (DOE's) Oak Ridge Field Research Center (FRC) at Oak Ridge, TN.

The Oak Ridge FRC is one of the most-studied sites for uranium bioremediation (2, 8, 19–22, 27, 37, 45–48). Previously used as a uranium enrichment plant, the site remains contaminated with depleted uranium, nitrate, and acidity. To deal with uranium contamination, dissimilatory metal reduction has been studied as an alternative that reduces risk by converting toxic soluble metals and radionuclides to insoluble, less toxic forms (2, 3, 16, 21, 26, 45). For example, some microbes can use metals such as Cr(VI), Se(VI), and the radionuclides U(VI) and Tc(VII) as final electron acceptors, producing a reduced insoluble species, thus blocking dispersal and reducing bioavailability.

* Corresponding author. Mailing address: Center for Microbial Ecology, Michigan State University, East Lansing, MI 48824-1325. Fax: (517) 353-2917. Phone for Terence L. Marsh: (517) 884-5391. E-mail: marsht@msu.edu. Phone for James M. Tiedje: (517) 353-9021. E-mail: tiedjej@msu.edu.

‡ Present address: Institute of Arctic Biology, University of Alaska Fairbanks, Fairbanks, AK 99775.

§ Present address: Soil & Crop Sciences Department, Texas A&M University, College Station, TX 77843-2474.

¶ Present address: Department of Civil & Environmental Engineering, Georgia Institute of Technology, Atlanta, GA 30332.

‖ Present address: Center for Critical Zone Research, Department of Plant and Soil Sciences, University of Delaware, Newark, DE 19711.

Present address: Department of Botany and Microbiology, University of Oklahoma, Norman, OK 73019.

† Supplemental material for this article may be found at http://aem.asm.org/.

▽ Published ahead of print on 20 August 2010.

The ability to reduce U(VI) to U(IV) has been found in several unrelated phylogenetic groups, i.e., *Delta-*, *Beta-*, *and Gammaproteobacteria*, *Firmicutes*, *Deinococci*, and *Actinobacteria*, among others (42). Most previous studies have focused on the Fe(III)-reducing bacteria (FRB), especially *Geobacter*, and the sulfate-reducing bacteria (SRB), especially *Desulfovibrio.* Uranium(VI) reduction for bioremediation purposes has been tested and confirmed in laboratory-scale experiments using serum bottles (13, 18, 48), microcosms (23, 32), sediment columns (14, 43), and *in situ* field studies (3, 21, 41, 45), with the last one demonstrating the feasibility of U(VI) remediation and the correlation of U(VI) reduction with FRB (3, 6, 18, 31, 41) or SRB (40), or both (8, 19, 49).

During field studies at Area 3 of the Oak Ridge site, a hydraulic control system together with ethanol injection successfully promoted U(VI) reduction from 5 μM to levels below U.S. Environmental Protection Agency (EPA) maximum contaminant levels (MCLs) for drinking water (0.126 μM) over a 2-year period (46). Reduction of U(VI) to U(IV) was confirmed by X-ray absorption near edge structure (XANES) (22, 46). Previous microbial surveys of sediments and groundwater from Area 3 wells by the use of 16S rRNA gene clone libraries detected genera known to harbor U(VI)-reducing members, such as *Geobacter*, *Desulfovibrio*, *Anaeromyxobacter*, *Desulfosporosinus*, and *Acidovorax*, after U(VI) reduction was established (8, 19). In one study, microbial counts from sediments were correlated with the hydraulic path, suggesting differences in organic carbon availability throughout Area 3 (8). The study that tracked the groundwater microbial communities of four locations of Area 3 over a 1.5-year period during ethanol stimulation found that nitrate, uranium, sulfide, and ethanol were correlated with particular bacterial populations and that the engineering control of dissolved oxygen and delivered nutrients was also significant in explaining the microbial community variability (19). However, the analysis of communities has been focused on limited wells and the community of the entire test area has not been characterized.

On the basis of the previous results, we further hypothesized that the hydrological control strategy employed for the remediation of the site constrained the geochemistry of the site by controlling the distribution of organic carbon substrates and other nutrients and that this in turn selected a characteristic microbial community that was distinguishable from its surrounding community. We used massively parallel sequencing of 16S rRNA genes from sediments of 15 wells to characterize the microbial communities along hydrological gradients from the microbiologically active and hydraulically protected inner-loop zone to less active and still contaminated areas outside the treatment area and downgradient. Our sediment-sampling strategy allows a more precise spatial characterization than the use of groundwater samples, where filtering large volumes of water is often required, and also because samples of the attached communities can differ from the planktonic ones, as expected in oligotrophic aquifers (15), such as this site. The deeper sequencing allowed a more extensive survey of the communities, higher confidence in the detection of less dominant but significant members, and a more statistically robust indicator species assessment. We were able to detect groups significantly associated with U(VI) reduction and to explain differences in community structure with hydrogeochemical conditions.

MATERIALS AND METHODS

Site description, hydraulic characterization, and sampling. Samples were retrieved from Area 3 of the DOE FRC at the Y-12 National Security Complex, Oak Ridge, TN, on 5 October 2005, after 775 days of treatment, as described previously (8). Briefly, sediments were withdrawn from wells by using a polyvinyl chloride surge block to draw the sediments surrounding the well screens into the well and were then pumped into glass bottles. The sediments were later separated from the slurry by centrifugation and frozen at −80°C, until their DNA was extracted (8). A hydraulic control system was established to control groundwater flow and to inject ethanol into the subsurface as an electron donor (45, 46). An outer groundwater recirculation loop (injection at well FW024, extraction at well FW103) protected an inner loop (injection at well FW104, extraction at well FW026) from penetration by highly contaminated groundwater from outside (Fig. 1). A downgradient well, well FW105 (6.63 m westwards of well FW103), was used to monitor the influence of the treatment on the geochemistry of groundwater that migrated to the downgradient (45). Multilevel sampling (MLS) wells FW100, FW101, and FW102 were used to monitor hydrogeology and remediation performance over seven different depths (depths −1 to −7). Injection and extraction wells were 14.6 m below ground (bg), with a screen being placed at between 11.28 and 13.77 m. MLS wells were sampled at 15.24, 13.7, 12.19, and 10.67 m bg for levels −1, −2, −3, and −4, respectively.

The remediation was initiated on 23 August 2003 (day 0), and during the first 137 days, groundwater was pumped, treated *ex situ* to adjust the pH and remove Al, Ca, and nitrate (via a denitrification bioreactor), and reinjected into the subsurface (20). Ethanol injection into the inner loop started on day 137 (46). The chemical oxygen demand (COD) concentration in groundwater was used as an indirect means to monitor the organic carbon electron donor in the subsurface. After biostimulation with weekly ethanol injections over a 2-year period, the uranium concentration in major MLS wells fell below EPA MCLs (46). The hydrology of the site was characterized by injecting a conservative tracer (bromide) together with ethanol (COD/Br^- ratio, 2.46 g/g) from days 801 to 803, as reported elsewhere (27). Two parameters from that study describe the connectivity of injection well FW104 to other wells and were used in this analysis: tracer recovery (the percentage of bromide from the injection site that reached each location sampled) and mean travel time (the time, in hours, for the tracer to travel from the injection site to each location sampled) (see Table S1 in the supplemental material). Recovery of the injected electron donor in each well was also estimated on the basis of the initial COD concentrations at injection well FW104 (see Table S1 in the supplemental material). The spatial distributions of bromide recovery ratios and mean travel times are shown in Fig. 1. Tracer recovery (percent) was a proxy for the potential amount of the stimulatory electron donor received at each location, and the mean travel time (from well FW104) was used as a proxy for the composition of the electron donor, since it has been demonstrated at this site that ethanol is converted to acetate by microbes as it moves thorough the aquifer.

Bioactivity of the wells was indicated by a combination of measures, including previously measured most probable numbers (MPNs) of FRB, SRB, and denitrifiers in the inner-loop wells (8) with levels of high tracer and COD recovery; Fe(II)/total Fe ratio; and the presence of sulfide and U(IV) in sediments and sulfide in groundwater (see Table S1 in the supplemental material). This information taken together allowed the wells to be grouped into three categories of high, medium, and low activity.

Chemicals and analytical methods. Chemical oxygen demand, sulfide, and Fe(II) were determined using a DR 2000 spectrophotometer (Hach Chemical, Loveland, CO). Anions (including NO_3^-, Cl^-, SO_4^{2-}, and PO_4^{3-}) were analyzed with an ion chromatograph, as described previously (8). Metals (Al, Ca, Fe, Mn, Mg, U, K, etc.) were determined by inductively coupled plasma mass spectrometry (Perkin-Elmer ELAN 6100 spectrometer), and the oxidation state of uranium was determined with XANES (23, 46). The proportion of Fe(II) to total Fe was measured as the HCl (10%)-extractable amount.

DNA extraction and direct sequencing. DNA was extracted from 0.5 g of well sediments with a Fast soil preparation kit (MoBio Inc., San Diego, CA), following the manufacturer's instructions. rRNA genes were amplified for pyrosequencing using a primer set that flanked the V4 hypervariable region of the 16S rRNA gene at corresponding *Escherichia coli* positions 563 and 802: primers 563F (5′-**GCCTCCCTCGCGCCATCAG**[bar code]AYTGGGYDTAAAGVG-3′) and 802R (5′-**GCCTTGCCAGCCCGCTCAG**TACNVGGGTATCTAATCC-3′), where the sequencing adaptors are in boldface. The forward primer additionally contained a short run of nucleotides used as bar codes. Bar codes were

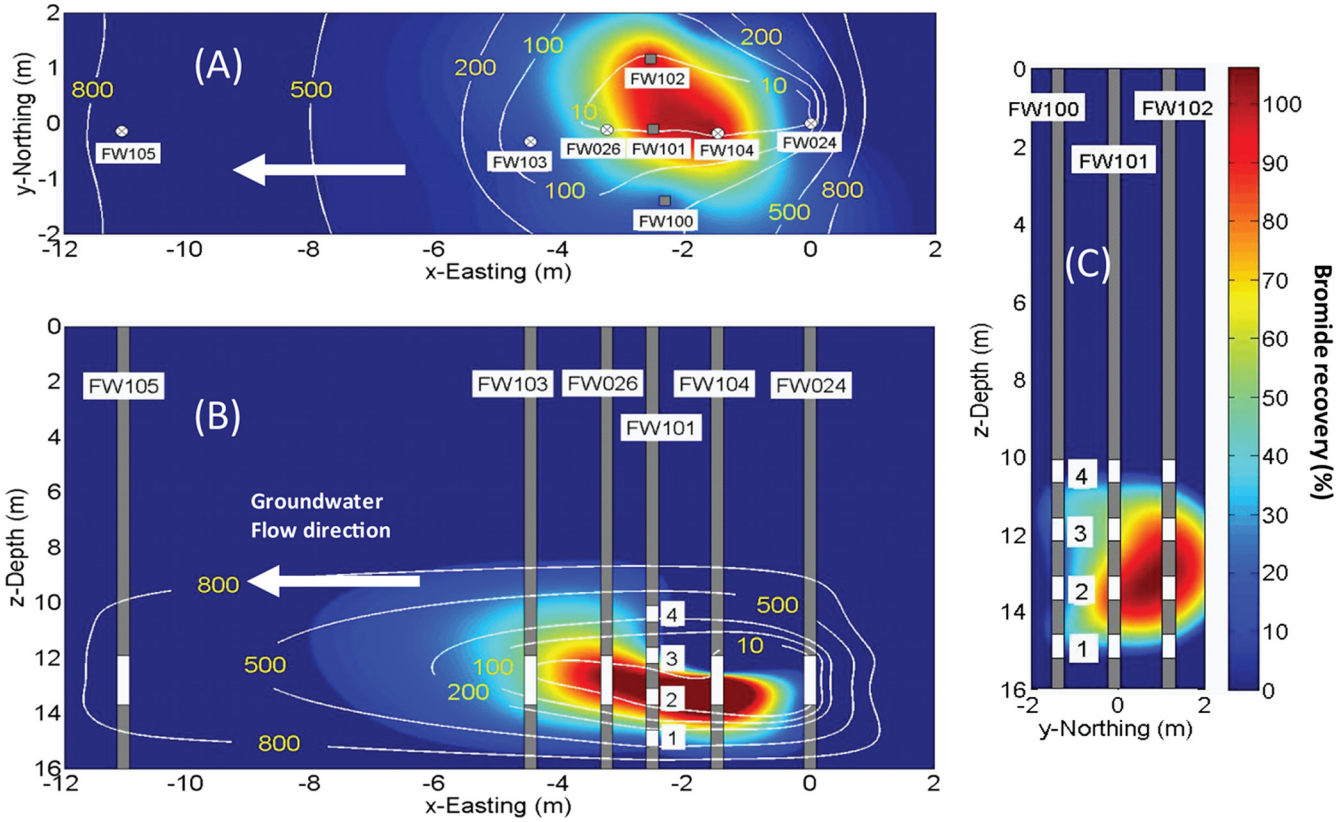

FIG. 1. Scheme of the well system in Area 3, Oak Ridge National Laboratory, DOE. Hydrology connectivity is shown with the spatial distributions of bromide recovery (as percent, in color) and mean travel times (contour lines with units of hours). (A) Horizontal plane at the 13-m depth below ground; (B) cross-vertical section along injection and extraction wells; (C) cross-vertical section along MLS wells. The horizontal distance (m) is measured from outer-loop injection well FW024 eastwards (x) or northwards (y). z is the depth below ground (m). The well system included inner-loop injection well FW104 and extraction well FW026 for ethanol injection, outer-loop injection well FW024 and extraction well FW103 for hydraulic protection, and downgradient well FW105. The multilevel sample wells are FW100, FW101, and FW102; and the −1, −2, −3, and −4 levels were used for monitoring. The electron donor (ethanol) was injected into the inner loop at well FW104.

distinct from each other by at least two nucleotides. Primers were dual high-pressure liquid chromatography purified (Integrated DNA Technologies, Coralville, IA). Each PCR mixture contained 1 μM each primer, 1.8 mM $MgCl_2$, 0.2 mM each deoxynucleoside triphosphate, 3 μg bovine serum albumin (New England Biolabs, Beverly, MA), 1 U of the FastStart high-fidelity PCR system enzyme blend (Roche Applied Science, Indianapolis, IN), and 10 ng of DNA template. DNA samples were amplified in triplicate using the following PCR conditions: 95°C for 3 min; 95°C for 45 s, 57°C for 45 s, and 72°C for 1 min for 30 cycles; and 72°C for 4 min. PCR products were separated in a 1% (wt/vol) agarose Tris-acetate-EDTA gel, and the bands between 270 and 300 bp were excised. Bands for each triplicate were pooled together, extracted with a QIAquick gel extraction kit (Qiagen Inc., Valencia, CA), cleaned for a second time with the QIAquick PCR purification kit (Qiagen Inc.), and eluted with 20 μl of EB buffer (10 mM Tris-Cl, pH 8.5). Clean products were quantified using an ND-1000 spectrophotometer (NanoDrop Technologies, Wilmington, DE) and mixed in equal amounts (20 ng each) for direct sequencing by a Genome Sequencer FLX system (454; Life Sciences).

Sequence processing. Sequences were processed with the Ribosomal Database Project (RDP) Pyrosequencing Pipeline (http://pyro.cme.msu.edu/index.jsp) (11). Sequences were first trimmed to remove the adaptor sequences and then sorted according to their bar codes, before the bar codes were removed. Quality filters removed sequences with lengths of less than 150 bases and those with more than two changes in the forward primer portion. No product smaller than 230 bases was expected when the product size was calculated using 7,449 nearly full-length sequences of type strains from the RDP. We used RDP's complete linkage clustering tool, a secondary-structure-based alignment based on the INFERNAL program (version 8.1), and a 16S rRNA secondary-structure model (7).

Data analysis. Sequences from different samples were classified using RDP's classifier with an 80% bootstrap confidence (44). Operational taxonomic units (OTUs) were defined at 5%. This level roughly corresponds to the genus-level boundary, according to the findings of a previous study that compared the average amino acid identities and 16S rRNA gene similarities of 410 sequenced genomes (24). The Sorensen index, as modified by Chao et al., was used to compare individual samples according to their diversity patterns (beta diversity analysis) (9). Clustering of samples was done by average-neighbor clustering. An indicator species approach was used on the resulting clustering topology to find groups that represent specific groups of samples (12). This method was chosen because it easily deals with the high number of sequences per sample and provides statistical support for the conclusions. An indicator value (range, 0 to 1) was generated for each OTU-sample cluster combination using both frequency of occurrence and relative abundance information, and a 1,000-bootstrap test was used to generate a P value for each indicator value (12). The indicator value for an OTU in a sample is high when that OTU is present in all the samples and highly abundant for that specific sample (12). Since we had 4,719 statistical tests, one for each OTU, there was a good chance of reporting false-positive results, i.e., using α equal to 0.05, $0.05 \times 4{,}719 = 234$ false-positive results. To avoid this issue, we used a false-discovery-rate (FRD) approach. The FDR estimates the chance of reporting a false-positive result in all the significant results (q value) and was used instead of the excessively conservative corrected P values (5). q values were generated from P values using the R program package QVALUE (version 1.0) (38, 39) with the bootstrap method setting. Significance was determined by using a q value of 0.05 (significant results have a less than 5% chance of being false positive by chance). Statistical analyses were conducted using the R environment (version 2.80; http://www.R-project.org.) with the packages Labdsv (version 1.3-1) (34) for indicator species analysis and QVALUE (version

1.1) for false-discovery-rate calculation (available at http://genomics.princeton.edu/storeylab/qvalue/) (38, 39).

Nucleotide sequence accession numbers. The sequences were submitted to the Sequence Read Archive (SRA) of the European Bioinformatics Institute (http://www.ebi.ac.uk) under SRA submission ERA010567, SRA project ERP000261, and SRA samples ERS012653 to ERS012669.

RESULTS

Geochemical and hydrological characterization of the site. Characterization of the test area showed significant differences in hydrology (connectivity to the injection site), geochemistry, and microbial activity (see Table S1 in the supplemental material). The differences were mostly connected to the presence of sulfate and iron, uranium metabolism, and electron donor availability. From these, uranium, sulfide, and tracer recovery are likely the most relevant to the microbial activities of the site because of their levels. Significantly more of the water injected at well FW104 reached inner-loop locations ($P < 0.01$) (Fig. 1A). MLS wells in inner-loop locations from levels −1 and −4 behaved more like those in outer-loop locations in terms of bioactivity, likely due to their poor connection to the injection well (Fig. 1B and C, *z* dimension). When the data for these wells are excluded, the mean travel time from injection well FW104 to the inner-loop wells was significantly shorter ($P < 0.05$) than that to the outer-loop ones. Inner-loop wells (except MLS wells at levels −1 and −4) showed high levels of bioactivity, relatively high Fe(II)/total iron ratios, sulfide presence, and some extent of U(IV) and thus high levels of bioactivity (see Table S1 in the supplemental material). Compared to the outer-loop wells, inner-loop wells had higher levels of tracer ($P < 0.01$) and COD ($P < 0.05$) recovery, and their water was richer in sulfide ($P < 0.01$) and iron ($P < 0.01$) and poorer in sulfate ($P < 0.05$). This trend remained when the findings for the inner-loop wells were compared to those for the downgradient area (well FW105), though no statistical comparison was possible (only one sample from the downgradient area existed). Clustering by chemical conditions (Fig. 2B) as well as visual patterns (Fig. 1) showed a clear separation of inner-loop wells of central depths (levels −2 and −3).

Microbial community structure. The 16S rRNA gene surveys produced a total of 97,610 sequences for 17 samples that covered three different conditions in the test area, including 10 samples from inner-loop wells, 8 samples from the outer loop, and 1 sample from the downgradient area. Each sample was covered by 6,498 ± 1,630 sequences. Two samples (samples from wells FW100-1 and FW101-1) yielded low sequence counts, and the data for the samples were discarded from the analysis; they were obtained from locations with low levels of connectivity (COD and tracer recovery) and bioactivity (see Table S1 in the supplemental material). Excluding the data for these samples, communities were generally dominated by a few OTUs; the 10 most abundant OTUs in any of our samples accounted for at least 40% of the sequences for that sample. No significant difference in richness was found between inner- and outer-loop locations.

Clustering of the samples on the basis of their microbial communities yielded four clusters (Fig. 2A) whose grouping was consistent with differences in the bioactivity and connectivity of the sampled area. Cluster L contained samples with low bioactivity and poor connectivity to the injection well

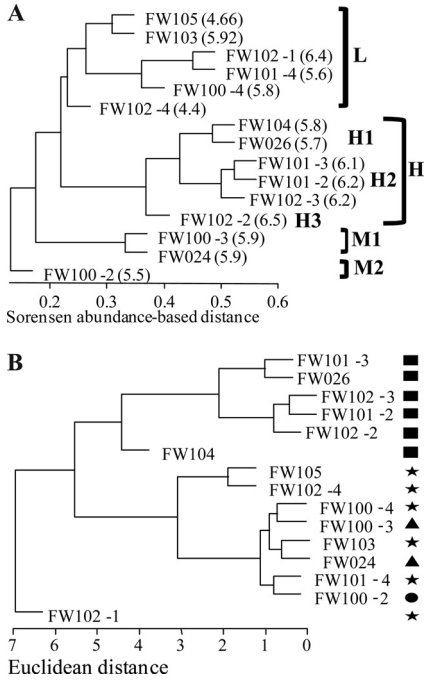

FIG. 2. Clustering of samples by geochemical and microbiological characteristics. (A) Clustering by microbial community structure using a Chao-Sorensen distance and average-neighbor algorithm. Samples grouped in four clusters: cluster L comprised wells with low levels of bioactivity and low levels of connectivity to the injection well. Cluster H has the most active communities and the highest connectivity. Clusters M1 and M2 contained wells with medium activity. In clusters H, M1, and M2, the subgroups seemed to be influenced by pH. The pH values for each well are also shown. (B) Clustering by geochemical composition. Colinear variables were eliminated after correlation analysis (data not shown); and only the data for pH, sulfate, nitrate, COD (as an indirect indicator of organic matter), and tracer recovery were used for analysis with a previous *z*-score transformation. Cluster affiliations by microbial community structure are marked as follows: ■, H cluster; ⋆, L cluster; ▲, M1 cluster; ●, M2 cluster. Hierarchical clustering used an average-neighbor algorithm.

(tracer recovery < 10%). Three samples from this group came from the inner-loop MLS wells at levels −1 and −4, where no electron donor was received (on the basis of tracer recovery, from Fig. 1C, and COD recovery, from Table S1 in the supplemental material). Cluster H contained all the samples with the highest bioactivity and where U(VI) reduction was observed. Clusters M1 and M2 were characterized by medium bioactivity. In these two MLS wells, the sediment samples contained reduced Fe(II) but no or extremely low levels of sulfide, and groundwater nitrate concentrations (0.017 and 0.023 mM) were much lower than those in other outer-loop MLS wells (1.6 to 1.9 mM) because a small fraction of organic electron donors reached these locations (COD recovery ≤ 5%; see Table S1 in the supplemental material).

Microbial communities were dominated by the classes *Proteobacteria* and *Acidobacteria* (see Fig. S1 in the supplemental material), consistent with the findings of previous clone library surveys of the site (8, 19). Differences in community structure among clusters of wells were mostly phyla of low abundance and specific *Proteobacteria* classes. On average, *Proteobacteria* and *Acidobacteria* together contributed 52% of the sequences.

TABLE 1. Indicator species of the L, M1, and M2 clusters[a]

Cluster affiliation	Indicator value	Classification[b]	Closest isolated relative[c] (GenBank accession no.)	Similarity[d]
L	0.985	*Castellaniella* (*Betaproteobacteria*)	*Castellaniella defragrans* 62Car (AJ005449)	1.00
L	0.941	*Rhodanobacter* (*Gammaproteobacteria*)	*Rhodanobacter ginsengisoli* GR17-7 (EF166075)	0.99
M1	0.968	Subdivision 3 (*Verrucomicrobia*)	Bacterium Ellin514 (AY960777)	0.95
M1	0.957	*OD1*	*Geobacter sulfurreducens* PCA (AE017180)	0.76
M1	0.900	U[e] *Bacteria*	*Xanthomonas axonopodis* XV338 (AF123090)	0.71
M1	0.900	U *Bacteria*	Chlorophyte isolate CMS93 (AJ880281)	0.92
M1	0.822	*Afipia* (*Alphaproteobacteria*)	*Lucina pectinata* gill symbiont (X84980)	0.81
M2	0.923	*Clostridiales* (*Firmicutes*)	*Bacteroides cellulosolvens*^{T} (L35517)	0.98

[a] $P = 0.001$ (1,000-bootstrap test in indicator species analysis), $q < 0.05$ (false discovery rate analysis of P values).
[b] Lowest classification indicated by RDP's classifier with an 80% bootstrap confidence.
[c] Closest relative determined by RDP Seqmatch using a good-quality, nearly full-length data set.
[d] Similarity is measured against its closest relative.
[e] U, undefined.

Proteobacteria contributed 39%, on average, with a maximum of 71% at well FW024 and a minimum of 18% at well FW100-2. *Acidobacteria* contributed 13% of the sequences, on average, with a maximum of 33% at well FW026 and minimum of 3% at well FW026. The *Actinobacteria* contribution was about 6% in all wells with the exception of one, well FW100-2, where its contribution was 36%.

When the four sample clusters are compared, cluster M2 was dominated by *Actinobacteria* and cluster M1 was dominated by *Proteobacteria*. Clusters L and H shared similar profiles; however, cluster H had significantly higher proportions of *Chloroflexi* ($P < 0.01$), *Chlamydiae* ($P < 0.01$), and *BRC1* ($P < 0.01$) than cluster L and significantly lower proportions of *Verrucomicrobia* ($P < 0.05$), *Actinobacteria* ($P < 0.05$), *TM7* ($P < 0.05$), and *Bacteroidetes* ($P < 0.05$) than cluster L.

The *Proteobacteria* composition varied the most across sites. When sample clusters H and L are compared, cluster H was enriched in *Deltaproteobacteria* ($P < 0.01$), while cluster L had a significantly higher proportion of *Gamma-* and *Alphaproteobacteria*. Given that the *Deltaproteobacteria* class has many of the known U(VI) reducers, such as *Geobacter* (*Desulfomoronales*), *Desulfovibrio* (*Desulfovibrionales*), and *Anaeromyxobacter* (*Myxococcales*), we evaluated if orders of this class were distributed in the same differential abundance in samples from active versus inactive wells. We found this to be true: the orders *Myxococcales* ($P = 0.01$), *Desulfobacterales* ($P < 0.05$), and *Desulfovibrionales* ($P < 0.01$) were enriched in high-activity wells compared with their levels in low-activity ones.

Indicator species for cluster L, H, and M wells. Abundance information for 4,719 OTUs over 15 samples was used to obtain indicator species representing the four sample clusters. *Rhodanobacter* (*Gammaproteobacteria*) and the denitrifying *Castellaniella* (*Betaproteobacteria*) were significant indicators for cluster L (Table 1). Nineteen OTUs were significant indicators of cluster H (Table 2), the only locations where U(VI) reduction was detected. Six of the OTUs belonged to known

TABLE 2. Indicator species of the H cluster of samples[a]

Indicator value	Classification[b]	Closest isolated relative[c] (GenBank accession no.)	Similarity[d]
1.000	*Desulfosporosinus* (*Firmicutes*)	*Desulfosporosinus* sp. strain 5apy (AF159120)	0.99
0.997	*Desulfosporosinus* (*Firmicutes*)	*Desulfosporosinus* sp. strain 5apy (AF159120)	0.99
0.980	U[e] *Burkholderiales* (*Betaproteobacteria*)	*Vogesella indigofera* ATCC 19706^T (AB021385)	0.96
0.977	U.*Peptococcaceae* (*Firmicutes*)	Anaerobic bacterium Prop2 (AY756143)	0.93
0.971	*Desulfosporosinus* (*Firmicutes*)	*Desulfosporosinus* sp. strain 5apy (AF159120)	0.98
0.970	*Desulfovibrio* (*Deltaproteobacteria*)	*Desulfovibrio putealis* DSM 16056^T (AY574979)	1.00
0.968	U *Firmicutes*	*Clostridium* sp. strain 9B4 (AY554416)	0.93
0.968	*Desulfovibrio* (*Deltaproteobacteria*)	Sulfate-reducing bacterium F1-7b (AJ012594)	1.00
0.959	U *BRC1*	Bacterium Ellin371 (AF498753)	0.83
0.948	*Anaeromyxobacter* (*Deltaproteobacteria*)	*Anaeromyxobacter dehalogenans* 2CP-1^T ATCC BAA-258^T (AF382396)	0.96
0.943	U *Alphaproteobacteria*	Endosymbiont of *Acanthamoeba polyphaga* (AF132138)	0.90
0.929	U *Betaproteobacteria*	*Gallionella ferruginea* subsp. *capsiferriformans* (DQ386262)	0.97
0.928	*Thiobacillus* (*Betaproteobacteria*)	*Thiobacillus sajanensis* 4HG (DQ390445)	0.99
0.906	U *Bacteria*	Spirochaetes bacterium SA-8 (AY695839)	0.87
0.890	*Chloroflexi*	*Leptolinea tardivitalis* YMTK-2^T (AB109438)	0.99
0.883	*Geothrix* (*Acidobacteria*)	*Geothrix fermentans* H5 (U41563)	0.98
0.866	U *Chlamydiales* (*Chlamydiae*)	*Chlamydiales* bacterium CRIB 32 (EU363464)	0.89
0.847	U *Betaproteobacteria*	*Ralstonia* sp. strain 22 (EU304284)	0.97
0.836	*Chloroflexi*	Bacterium K-4b6 (AF524858)	0.96

[a] $P = 0.001$ (1,000-bootstrap test in indicator species analysis), $q < 0.05$ (false discovery rate analysis of P values).
[b] Lowest classification indicated by RDP's classifier with an 80% bootstrap confidence.
[c] Closest relative determined by RDP Seqmatch using a good-quality, nearly full-length data set.
[d] Similarity is measured against its closest relative.
[e] U, undefined.

U(VI)-reducing genera: three *Desulfosporosinus* spp. (SRB *Firmicutes*), two *Desulfovibrio* spp. (SRB *Deltaproteobacteria*), and one *Anaeromyxobacter* sp. (FRB *Deltaproteobacteria*). Additionally, one OTU belonged to the *Peptococcaceae*, a family that harbors the U(VI) reducers *Desulfosporosinus* and *Desulfitobacterium*. Another three significant indicators were known to reduce or oxidize Fe(II) ⇆ Fe(III): *Thiobacillus*, *Geothrix*, and *Gallionella.* Other Fe(III) reducers, such as *Geobacter* and *Ferribacterium*, showed high indicator values, although they were not significant after the false discovery rate was applied.

In cluster H, one OTU belonged to the *Chlamydiales* class, a group mostly known to harbor intracellular pathogens; however, the OTU did not cluster with the human pathogens but clustered with the amoeba endosymbionts (data not shown). An additional significant OTU was also related to a known amoeba endosymbiont that clusters in the *Alphaproteobacteria.* In both cases, the similarity to isolates was not high (~90%), but the similarity to environmental clone sequences was 98%. Since the level of biomass growth in the active wells was high, the presence of predatory amoebae could explain the abundance patterns of these two groups.

Clusters M1, with five significant indicators, and M2, with one significant indicator, did not contain indicator species from known U(VI)-reducing genera (Table 1). Cluster M1 indicators mostly belong to poorly studied groups, such as *Verrucomicrobia* and *OD1*. Two of these indicator species were not classifiable with more than 80% confidence to any phylum of the RDP taxonomy. The significant indicator species from cluster M2 belonged to the *Clostridiales* order, with no lower-level classification being possible.

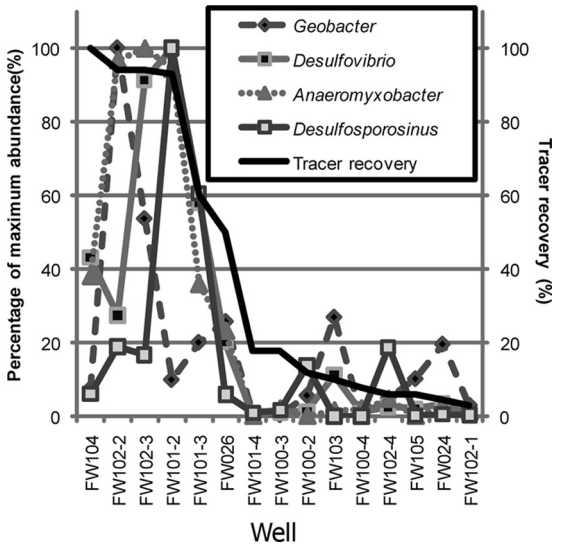

FIG. 3. Location of maximum abundance for uranium-reducing genera along the connectivity gradient. Since relative abundances among the different groups varied by up to 20 times, the ratios of abundance to the maximum abundance for the selected group (percent) are plotted. Tracer recovery values (percent) at each well are also presented.

DISCUSSION

In the present study we used massive parallel sequencing to test the hypothesis that aquifer zones that showed high connectivity to the electron donor source selected for similar communities that were different from the original and that these communities contained statistically supported indicator species that were potentially related to bioremediation at the site. Furthermore, the much deeper sequencing more strongly supports the conclusion that SRB especially and some FRB responded to the treatment and were prevalent in the active zones where U(VI) bioreduction occurred.

The bacterial community structure of the wells showed patterns that could be explained by the connectivity between the sampling locations and the electron donor injection well. Further analysis found significant indicator populations when their abundance patterns were compared. Groups specific to the low-bioactivity wells (cluster L) were closely related to isolates known to resist stress caused by low pH and high nitrate levels. In a similar fashion, groups in the high-bioactivity wells (cluster H) were closely related to known U(VI) reducers. Cluster L was characterized by *Rhodanobacter* and *Castellaniella*. The former was previously detected by 16S rRNA gene surveys (8) and by a metagenome of groundwater from well FW106, an untreated control location 9.9 m southward from the treatment zone. This well had a 3.6 pH and high levels of nitrate (38 to 54 mM) and uranium (110 to 130 μM). The metagenome revealed part of a *Rhodanobacter* genome with a wide variety of metal resistance genes and indications that these genes were horizontally transferred (17). A *Castellaniella* sp., a denitrifying member of the *Betaproteobacteria*, was previously found in groundwater of biostimulated (by injection of ethanol and bicarbonate) wells at Area 1 of FRC (a location also acidic and contaminated with nitrate and uranium), where it was the dominant *nirK*-containing denitrifier (37). *Castellaniella* was isolated from that site under acidic (pH 4.5) and neutral (pH 7.5) culture conditions, suggesting that it has an advantage over other denitrifiers under acidic conditions typical of the FRC contaminated areas (37). *Castellaniella* has also been detected in microcosm enrichments from FRC Area 2 (1).

Indicator species from bioactive wells were mostly known U(VI) reducers, Fe(III) reducers, or Fe(II) oxidizers. In general, the uranium content (200 to 1,000 mg/kg) in subsurface sediments prior to biostimulation of samples should not be enough to support microbial growth, due to poor bioavailability, especially in its uranyl phosphate form (22), but the iron content of up to 3 to 5% (wt/wt) should be enough (14). The appearance of U(VI)-reducing bacteria is not likely dependent only on the presence of U(VI) but more likely is related to reduction of other electron acceptors, such as Fe(III) and sulfate, resulting in a community capable of reducing U(VI) to U(IV). Five of the six known U(VI)-reducing indicator species were SRB (*Desulfovibrio* and *Desulfosporosinus*), suggesting that SRB may play a greater role in U(VI) reduction. Even though other possible U(VI) reducers were detected in cluster H (*Geobacter*, *Clostridium*) or even in other clusters (*Acidovorax*, *Clostridium*, *Deinococcus*), they did not show an abundance pattern that significantly associated them with U(VI) reduction. This was especially surprising for *Geobacter*, since its pattern of abundance, as well as the patterns of some other U(VI) reducers, correlated with gradients in connectivity, as measured by tracer recovery (Fig. 3). *Geothrix*, an FRB member of the

Acidobacteria, has been found in FRC sediments with bioreduced U(VI) in previous studies (6, 8), although no report has shown that it reduces U(VI) to U(IV) in pure culture. *Thiobacillus*, a member of the *Betaproteobacteria*, was also previously found at the FRC and is mostly known for its ability to oxidize sulfur compounds aerobically. *Thiobacillus denitrificans* is also capable of reducing nitrate to N_2 while oxidizing Fe(II) to Fe(III) or uranium(IV) to U(VI) (4). Its presence at the top of the indicator list suggests that it may play a role in Fe(III) reduction/reoxidation and U(VI) reduction in the presence of an iron or sulfur source and that it may influence the mobility of uranium if nitrate invades the bioreduced area. The presence of *Thiobacillus* spp. was also observed in a static microcosm test over an 11-month period under anaerobic conditions (23). Furthermore, a recent study confirmed that genes of *Thiobacillus* spp. increased after the U(VI) bioreduced site was reoxidized by nitrate (47).

At the initial period of biostimulation (day 278), FRB levels (measured by MPN) were 10 times higher than SRB levels in MLS wells (46) but then they declined, and at the sampling date for the present study (day 774), SBR were 10- to 100-fold more abundant than FRB (8). This is likely due to the decrease in bioavailability of the Fe(III) source from the sediments as the electron acceptor for FRB growth but no limitation for sulfate coming from groundwater flow. A similar trend for limitation of FRB was also observed at the DOE Rifle site when acetate was used as the electron donor (3) and for a static microcosm test with FRC sediments, which showed up to 80% U(VI) reduction to U(IV) but more than 50% of the ferrihydrite remaining intact even after a 5-month biostimulation with hydrogen (23). In both cases, SRB become predominant.

Since FRB can survive outside the treatment area, their pattern of abundance may not have been specific to U(VI) reduction and, hence, nonsignificant by our analysis. Thus, their participation in U(VI) reduction cannot be ruled out. The presence of members of the *Chloroflexi*, some of which are common in carbon-rich, anaerobic decomposing communities, and two putative endosymbionts of *Acanthamoeba*, a common free-living protozoon that feeds on bacteria (28), can be explained by the high levels of microbial biomass, as evidenced by occasionally clogged wells (46).

The high abundance of *Desulfovibrio* and *Desulfosporosinus* at the wells with low U(VI) levels and high SRB MPNs (up to 1.53×10^8 cell/g sediment; see reference 8) does not exclude the possibility that FRB contributed to U(VI) reduction, even though their abundance pattern did not reach the statistical threshold or that acetate (their most likely available electron donor) provides less energy than ethanol. Several FRB were significantly associated with cluster H, and at least one study showed an association between *Geobacter* and U(VI) reduction in columns packed with FRC Area 2 sediments (46). *Geothrix* and *Ferribacterium* have been associated with U(VI) reduction in other studies with reduced FRC sediments or groundwater, though no direct evidence of U(VI) reduction by them exists to date (6, 8, 19). A possibility that remains unexplored is that some of these FRB, e.g., *Ferribacterium*, *Geobacter*, and *Geothrix*, indirectly contribute to U(VI) reduction by their known ability to produce bioreduced compounds capable of reducing U(VI) to U(IV) abiotically, such as reduced iron compounds and humic acids (10, 30, 33). Competition for Fe(III) by FRB, which would decrease the relative abundance of *Geobacter*, may also explain why it was not significantly associated with U(VI) reduction.

The composition of the available organic carbon, mostly ethanol, at the injection site and acetate in the monitoring wells also explains the dominance of SRB over FRB, since the dominant FRB are mostly known not to use ethanol but the dominant SRB present are known to do so.

The presence of Fe(II) oxidizers in the high-bioactivity areas and their specific pattern of abundance suggest that they are active and could influence the bioremediation of the site. This is potentially the case for *Thiobacillus*, a Fe(II) oxidizer that can also anaerobically oxidize U(IV), with nitrate being the final electron acceptor (4).

Our results fit a situation where SRB have a predominant role in U(VI) reduction at the FRC site when U reached levels below EPA MCLs because (i) the majority of significant U(VI) reducers detected in cluster H were SRB (*Desulfovibrio*, *Desulfosporosinus*) and SRB were the dominant population by MPN (8); (ii) the pattern of ethanol oxidation to acetate was consistent with ethanol metabolism by SRB such as *Desulfovibrio* and *Desulfosporosinus* (25, 35); (iii) the results of FRC field tests indicated that when ethanol was used as the electron donor, sulfate and U(VI) reduction occurred simultaneously (1, 29, 46); (iv) *Desulfovibrio* was previously detected in pretreatment bioreactors fed with FRC water and stimulated with ethanol and lactate and where U(VI) reduction was confirmed (20, 48); (v) SRB were also present at low levels in the treated water from an on-site bioreactor that treated groundwater which was later reinjected into the contaminated aquifer (48); and (vi) alternative electron acceptors are more accessible to SRB than FRB, since sulfate was always present in groundwater, while the availability of ferric(hydro) oxides was poor and could eventually become limited (mostly mineral bound).

Our pyrosequencing approach potentially avoided a cloning bias shown for rRNA genes cloned into a host such as *E. coli* (36) and allowed us to explore more deeply the microbial diversity of the site, obtaining 100 times more sequences at half the price (in comparison with the number of sequences and the price of our previous clone library studies). With this method we were able to survey enough locations along the gradients in the test area to ensure a high confidence in the significance of the association of bacterial groups to the bioactive area with U(VI) reduction. We were also able to find previously undetected U(VI) reducers (e.g., *Shewanella*) and groups that have a significant abundance pattern that associates them with U(VI) reduction but whose levels in clone libraries were low enough to be undetected or poorly understood, with the latter being the case for *Anaeromyxobacter*, an Fe(III) and U(VI) reducer that was present at low levels (~0.5%) and that was mostly undetected in previous clone library studies (8).

ACKNOWLEDGMENTS

This study was funded by the U.S. Department of Energy's Office of Science under grants DE-FG02-97ER62469 and DE-FG02-97ER64398 for the microbial studies and grant C05-00OR22725 for the field work. Mary Beth Leigh was supported by a U.S. National Science Foundation postdoctoral fellowship.

We thank Hui Yan, Kenneth Lowe, and Tonia Mehlhorn for help with field tests and analytic work and James Cole, Benli Chai, and

Qiong Wang from the Ribosomal Database Project for their help with the pyrosequence analysis.

REFERENCES

1. **Akob, D. M., H. J. Mills, T. M. Gihring, L. Kerkhof, J. W. Stucki, A. S. Anastacio, K. J. Chin, K. Kusel, A. V. Palumbo, D. B. Watson, and J. E. Kostka.** 2008. Functional diversity and electron donor dependence of microbial populations capable of U(VI) reduction in radionuclide-contaminated subsurface sediments. Appl. Environ. Microbiol. **74:**3159–3170.
2. **Anderson, R. T.** 2006. DOE genomics: applications to *in situ* subsurface bioremediation. Remediation J. **17:**23–38.
3. **Anderson, R. T., H. A. Vrionis, I. Ortiz-Bernad, C. T. Resch, P. E. Long, R. Dayvault, K. Karp, S. Marutzky, D. R. Metzler, A. Peacock, D. C. White, M. Lowe, and D. R. Lovley.** 2003. Stimulating the in situ activity of *Geobacter* species to remove uranium from the groundwater of a uranium-contaminated aquifer. Appl. Environ. Microbiol. **69:**5884–5891.
4. **Beller, H. R.** 2005. Anaerobic, nitrate-dependent oxidation of U(IV) oxide minerals by the chemolithoautotrophic bacterium *Thiobacillus denitrificans*. Appl. Environ. Microbiol. **71:**2170–2174.
5. **Benjamini, Y., and Y. Hochberg.** 1995. Controlling the False discovery rate: a practical and powerful approach to multiple testing. J. R. Stat. Soc. B **57:**289–300.
6. **Brodie, E. L., T. Z. Desantis, D. C. Joyner, S. M. Baek, J. T. Larsen, G. L. Andersen, T. C. Hazen, P. M. Richardson, D. J. Herman, T. K. Tokunaga, J. M. Wan, and M. K. Firestone.** 2006. Application of a high-density oligonucleotide microarray approach to study bacterial population dynamics during uranium reduction and reoxidation. Appl. Environ. Microbiol. **72:**6288–6298.
7. **Cannone, J. J., S. Subramanian, M. N. Schnare, J. R. Collett, L. M. D'Souza, Y. Du, B. Feng, N. Lin, L. V. Madabusi, K. M. Muller, N. Pande, Z. Shang, N. Yu, and R. R. Gutell.** 2002. The comparative RNA web (CRW) site: an online database of comparative sequence and structure information for ribosomal, intron, and other RNAs. BMC Bioinformatics **3:**2.
8. **Cardenas, E., W. M. Wu, M. B. Leigh, J. Carley, S. Carroll, T. Gentry, J. Luo, D. Watson, B. Gu, M. Ginder-Vogel, P. K. Kitanidis, P. M. Jardine, J. Zhou, C. S. Criddle, T. L. Marsh, and J. M. Tiedje.** 2008. Microbial communities in contaminated sediments, associated with bioremediation of uranium to submicromolar levels. Appl. Environ. Microbiol. **74:**3718–3729.
9. **Chao, A., R. L. Chazdon, R. K. Colwell, and T. J. Shen.** 2006. Abundance-based similarity indices and their estimation when there are unseen species in samples. Biometrics **62:**361–371.
10. **Coates, J. D., D. J. Ellis, C. V. Gaw, and D. R. Lovley.** 1999. *Geothrix fermentans* gen. nov., sp. nov., a novel Fe(III)-reducing bacterium from a hydrocarbon-contaminated aquifer. Int. J. Syst. Bacteriol. **49**(Pt. 4)**:**1615–1622.
11. **Cole, J. R., Q. Wang, E. Cardenas, J. Fish, B. Chai, R. J. Farris, A. S. Kulam-Syed-Mohideen, D. M. McGarrell, T. Marsh, G. M. Garrity, and J. M. Tiedje.** 2009. The Ribosomal Database Project: improved alignments and new tools for rRNA analysis. Nucleic Acids Res. **37:**D141–D145.
12. **Dufrene, M., and P. Legendre.** 1997. Species assemblages and indicator species: the need for a flexible asymmetrical approach. Ecol. Monogr. **67:**345–366.
13. **Finneran, K. T., M. E. Housewright, and D. R. Lovley.** 2002. Multiple influences of nitrate on uranium solubility during bioremediation of uranium-contaminated subsurface sediments. Environ. Microbiol. **4:**510–516.
14. **Gu, B., W. M. Wu, M. A. Ginder-Vogel, H. Yan, M. W. Fields, J. Zhou, S. Fendorf, C. S. Criddle, and P. M. Jardine.** 2005. Bioreduction of uranium in a contaminated soil column. Environ. Sci. Technol. **39:**4841–4847.
15. **Hazen, T., L. Jiménez, G. López de Victoria, and C. Fliermans.** 1991. Comparison of bacteria from deep subsurface sediment and adjacent groundwater. Microb. Ecol. **22:**293–304.
16. **Hazen, T. C., and H. H. Tabak.** 2005. Developments in bioremediation of soils and sediments polluted with metals and radionuclides. 2. Field research on bioremediation of metals and radionuclides. Rev. Environ. Sci. Biotechnol. **4:**157–183.
17. **Hemme, C. L., Y. Deng, T. J. Gentry, M. W. Fields, L. Wu, S. Barua, K. Barry, S. G. Tringe, D. B. Watson, Z. He, T. C. Hazen, J. M. Tiedje, E. M. Rubin, and J. Zhou.** 2010. Metagenomic insights into evolution of a heavy metal-contaminated groundwater microbial community. ISME J. **4:**660–672.
18. **Holmes, D. E., K. T. Finneran, R. A. O'Neil, and D. R. Lovley.** 2002. Enrichment of members of the family *Geobacteraceae* associated with stimulation of dissimilatory metal reduction in uranium-contaminated aquifer sediments. Appl. Environ. Microbiol. **68:**2300–2306.
19. **Hwang, C., W. Wu, T. J. Gentry, J. Carley, G. A. Corbin, S. L. Carroll, D. B. Watson, P. M. Jardine, J. Zhou, C. S. Criddle, and M. W. Fields.** 2009. Bacterial community succession during in situ uranium bioremediation: spatial similarities along controlled flow paths. ISME J. **3:**47–64.
20. **Hwang, C., W. M. Wu, T. J. Gentry, J. Carley, S. L. Carroll, C. Schadt, D. Watson, P. M. Jardine, J. Zhou, R. F. Hickey, C. S. Criddle, and M. W. Fields.** 2006. Changes in bacterial community structure correlate with initial operating conditions of a field-scale denitrifying fluidized bed reactor. Appl. Microbiol. Biotechnol. **71:**748–760.
21. **Istok, J. D., J. M. Senko, L. R. Krumholz, D. Watson, M. A. Bogle, A. Peacock, Y. J. Chang, and D. C. White.** 2004. In situ bioreduction of technetium and uranium in a nitrate-contaminated aquifer. Environ. Sci. Technol. **38:**468–475.
22. **Kelly, S. D., K. M. Kemner, J. Carley, C. Criddle, P. M. Jardine, T. L. Marsh, D. Phillips, D. Watson, and W.-M. Wu.** 2008. Speciation of uranium in sediments before and after in situ biostimulation. Environ. Sci. Technol. **42:**1558–1564.
23. **Kelly, S. D., W. M. Wu, F. Yang, C. S. Criddle, T. L. Marsh, E. J. O'Loughlin, B. Ravel, D. Watson, P. M. Jardine, and K. M. Kemner.** 2010. Uranium transformations in static microcosms. Environ. Sci. Technol. **44:**236–242.
24. **Konstantinidis, K. T., and J. M. Tiedje.** 2007. Prokaryotic taxonomy and phylogeny in the genomic era: advancements and challenges ahead. Curr. Opin. Microbiol. **10:**504–509.
25. **Krieg, N. R., and J. G. Holt.** 1984. Bergey's manual of systematic bacteriology. The Williams & Wilkins Co., Baltimore, MD.
26. **Lovley, D. R., E. J. P. Phillips, Y. A. Gorby, and E. R. Landa.** 1991. Microbial reduction of uranium. Nature **350:**413–416.
27. **Luo, J., W.-M. Wu, J. Carley, C. Ruan, B. Gu, P. M. Jardine, C. S. Criddle, and P. K. Kitanidis.** 2007. Hydraulic performance analysis of a multiple injection-extraction well system. J. Hydrol. **336:**294.
28. **Marciano-Cabral, F., and G. Cabral.** 2003. *Acanthamoeba* spp. as agents of disease in humans. Clin. Microbiol. Rev. **16:**273–307.
29. **Michalsen, M. M., B. A. Goodman, S. D. Kelly, K. M. Kemner, J. P. McKinley, J. W. Stucki, and J. D. Istok.** 2006. Uranium and technetium bio-immobilization in intermediate-scale physical models of an in situ biobarrier. Environ. Sci. Technol. **40:**7048–7053.
30. **Nevin, K. P., and D. R. Lovley.** 2000. Potential for nonenzymatic reduction of Fe(III) via electron shuttling in subsurface sediments. Environ. Sci. Technol. **34:**2472–2478.
31. **North, N. N., S. L. Dollhopf, L. Petrie, J. D. Istok, D. L. Balkwill, and J. E. Kostka.** 2004. Change in bacterial community structure during in situ biostimulation of subsurface sediment cocontaminated with uranium and nitrate. Appl. Environ. Microbiol. **70:**4911–4920.
32. **Nyman, J. L., T. L. Marsh, M. A. Ginder-Vogel, M. Gentile, S. Fendorf, and C. Criddle.** 2006. Heterogeneous response to biostimulation for U(VI) reduction in replicated sediment microcosms. Biodegradation **17:**303–316.
33. **O'Loughlin, E. J., S. D. Kelly, R. E. Cook, R. Csencsits, and K. M. Kemner.** 2003. Reduction of uranium(VI) by mixed iron(II)/iron(III) hydroxide (green rust): formation of UO_2 nanoparticles. Environ. Sci. Technol. **37:**721–727.
34. **Roberts, D. W.** 2007. Labdsv: ordination and multivariate analysis for ecology. R package v1.3–1. http://cran.r-project.org/web/packages/labdsv/index.html.
35. **Robertson, W. J., J. P. Bowman, P. D. Franzmann, and B. J. Mee.** 2001. *Desulfosporosinus meridiei* sp. nov., a spore-forming sulfate-reducing bacterium isolated from gasolene-contaminated groundwater. Int. J. Syst. Evol. Microbiol. **51:**133–140.
36. **Sorek, R., Y. Zhu, C. J. Creevey, M. P. Francino, P. Bork, and E. M. Rubin.** 2007. Genome-wide experimental determination of barriers to horizontal gene transfer. Science **318:**1449–1452.
37. **Spain, A. M., A. D. Peacock, J. D. Istok, M. S. Elshahed, F. Z. Najar, B. A. Roe, D. C. White, and L. R. Krumholz.** 2007. Identification and isolation of a *Castellaniella* species important during biostimulation of an acidic nitrate- and uranium-contaminated aquifer. Appl. Environ. Microbiol. **73:**4892–4904.
38. **Storey, J., J. Taylor, and D. Siegmund.** 2004. Strong control, conservative point estimation and simultaneous conservative consistency of false discovery rates: a unified approach. J. R. Statist. Soc. B **66:**187–205.
39. **Storey, J., and R. Tibshirani.** 2003. Statistical significance for genomewide studies. Proc. Natl. Acad. Sci. U. S. A. **100:**9440–9445.
40. **Suzuki, Y., S. D. Kelly, K. M. Kemner, and J. F. Banfield.** 2003. Microbial populations stimulated for hexavalent uranium reduction in uranium mine sediment. Appl. Environ. Microbiol. **69:**1337–1346.
41. **Vrionis, H. A., R. T. Anderson, I. Ortiz-Bernad, K. R. O'Neill, C. T. Resch, A. D. Peacock, R. Dayvault, D. C. White, P. E. Long, and D. R. Lovley.** 2005. Microbiological and geochemical heterogeneity in an in situ uranium bioremediation field site. Appl. Environ. Microbiol. **71:**6308–6318.
42. **Wall, J. D., and L. R. Krumholz.** 2006. Uranium reduction. Annu. Rev. Microbiol. **60:**149–166.
43. **Wan, J., T. K. Tokunaga, E. Brodie, Z. Wang, Z. Zheng, D. Herman, T. C. Hazen, M. K. Firestone, and S. R. Sutton.** 2005. Reoxidation of bioreduced uranium under reducing conditions. Environ. Sci. Technol. **39:**6162–6169.
44. **Wang, Q., G. M. Garrity, J. M. Tiedje, and J. R. Cole.** 2007. Naive Bayesian classifier for rapid assignment of rRNA sequences into the new bacterial taxonomy. Appl. Environ. Microbiol. **73:**5261–5267.
45. **Wu, W. M., J. Carley, M. Fienen, T. Mehlhorn, K. Lowe, J. Nyman, J. Luo, M. E. Gentile, R. Rajan, D. Wagner, R. F. Hickey, B. Gu, D. Watson, O. A. Cirpka, P. K. Kitanidis, P. M. Jardine, and C. S. Criddle.** 2006. Pilot-scale in situ bioremediation of uranium in a highly contaminated aquifer. 1. Conditioning of a treatment zone. Environ. Sci. Technol. **40:**3978–3985.
46. **Wu, W. M., J. Carley, T. Gentry, M. A. Ginder-Vogel, M. Fienen, T. Mehl-**

horn, H. Yan, S. Caroll, M. N. Pace, J. Nyman, J. Luo, M. E. Gentile, M. W. Fields, R. F. Hickey, B. Gu, D. Watson, O. A. Cirpka, J. Zhou, S. Fendorf, P. K. Kitanidis, P. M. Jardine, and C. S. Criddle. 2006. Pilot-scale in situ bioremediation of uranium in a highly contaminated aquifer. 2. Reduction of U(VI) and geochemical control of U(VI) bioavailability. Environ. Sci. Technol. **40:**3986–3995.

47. **Wu, W. M., J. Carley, S. J. Green, J. Luo, S. D. Kelly, J. V. Nostrand, K. Lowe, T. Mehlhorn, S. Carroll, B. Boonchayanant, F. E. Loffler, D. Watson, K. M. Kemner, J. Zhou, P. K. Kitanidis, J. E. Kostka, P. M. Jardine, and C. S. Criddle.** 2010. Effects of nitrate on the stability of uranium in a bioreduced region of the subsurface. Environ. Sci. Technol. **44:**5104–5111.
48. **Wu, W. M., B. Gu, M. W. Fields, M. Gentile, Y. K. Ku, H. Yan, S. Tiquias, T. Yan, J. Nyman, J. Zhou, P. M. Jardine, and C. S. Criddle.** 2005. Uranium (VI) reduction by denitrifying biomass. Bioremediation J. **9:**46–61.
49. **Xu, M., W. M. Wu, L. Wu, Z. He, J. D. Van Nostrand, Y. Deng, J. Luo, J. Carley, M. Ginder-Vogel, T. J. Gentry, B. Gu, D. Watson, P. M. Jardine, T. L. Marsh, J. M. Tiedje, T. Hazen, C. S. Criddle, and J. Zhou.** 2010. Responses of microbial community functional structures to pilot-scale uranium in situ bioremediation. ISME J. **4:**1060–1070.